

Thin liquid layers supported by steady air-flow surface traction

By A. C. KING¹ AND E. O. TUCK²

¹Department of Mathematics, University of Keele, Staffs FT5 5BG, UK

²Applied Mathematics Department, University of Adelaide, S.A. 5001, Australia

(Received 1 October 1991 and in revised form 23 November 1992)

Upward flow of air can support a thin layer of liquid on a plane wall against gravity. Such apparently stationary layers are for example sometimes seen on the windscreen of a car travelling at high speed in rain. We solve here the two-dimensional case of a layer whose length is finite, but significantly greater than the meniscus length. The flow is steady, with a fixed layer boundary, inside which there is a steadily circulating viscous liquid, and outside which the air exerts a traction which is assumed to have a known (small) constant drag coefficient C_D . The air also exerts a non-uniform pressure on the liquid layer, of a magnitude determined by the shape of the layer, and the relationship between these two quantities can be obtained by thin-airfoil theory. In the lubrication approximation, the problem can be reduced to a nonlinear singular integro-differential equation to determine the unknown shape of the layer boundary. This equation is solved numerically for various (small) wall angles, for cases where the effect of surface tension is confined to a small meniscus region near the layer's leading edge. The numerical results indicate that solutions exist only for walls whose inclination is less than $0.70 C_D^{1/2}$, and, for a range of inclinations below that maximum value, that two distinct steady solutions can exist at each inclination.

1. Introduction

Consider the flow illustrated in figure 1. A quantity of viscous liquid of density ρ_w lies on a plane wall, which in general is not horizontal. The liquid mass is prevented from sliding down the plane by an upward stream of air of density ρ_A which exerts a tangential stress on its surface. We seek steady solutions with a surface $y = h(x)$ independent of time t .

The tangential stress cannot, however, overcome gravity g throughout the liquid layer, and we must expect that the liquid will be in motion, those particles near the layer's surface moving upward with the surface traction, whereas those particles near the middle of the layer's thickness move down with gravity. Hence we expect a slow rotational steady flow within the layer.

The liquid layer is assumed to be thin. In fact, we shall see that its mean slope, or thickness-to-length ratio ϵ , is of the order of the square root of the drag coefficient of the air flow, and the latter is small in the situations of interest here. Our theory is thus asymptotic for small ϵ . If, as we also assume, the Reynolds number of the motion in the layer is not too large (specifically smaller than the order of ϵ^{-2}), the conditions for lubrication theory to be valid are met for that flow.

We assume that the tangential stress is constant in magnitude over the layer. This will be the case if the whole layer consists of a thin drop which occupies only a small portion of the area of a solid surface exposed to an air flow. The appropriate choice

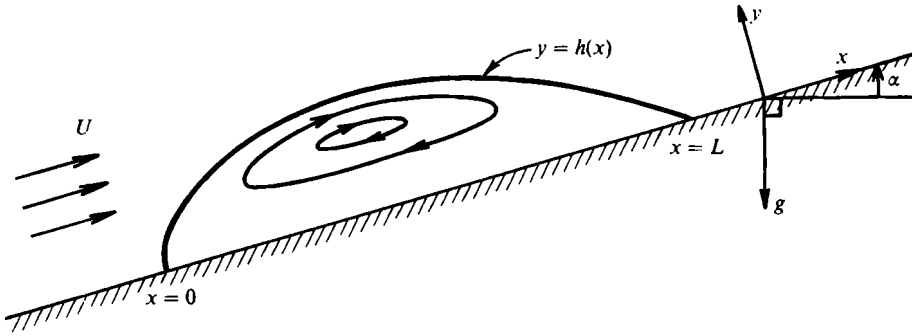


FIGURE 1. Definition sketch of a surface-traction-supported fluid drop.

for the constant tangential stress is then that for the local stress at the location of the drop in the boundary layer for that air flow, evaluated at the surface of the solid body as if the drop were absent, since the drop is thin. This condition of constancy of the tangential stress over the layer's surface can be relaxed in a more general model of larger layers, but we retain it in the present work, as a first approximation which captures the essential supporting role of the air flow.

The air stream not only provides a tangential stress, but also exerts a normal stress. This would be dynamically insignificant if it were constant, as it would be for a uniform (effectively inviscid and hence slipping) air flow over a plane wall. Hence, to fully account for the air stream, we need also to include a non-constant pressure distribution, which depends upon the shape $h(x)$ of the surface over which the air flow takes place. This dependence can be determined using thin-airfoil theory.

When we combine the (nonlinear differential) equations of lubrication theory with the (linear singular integral) equations of thin-airfoil theory, a nonlinear singular integro-differential equation for $h(x)$ results. This equation can take various forms depending on further geometrical and physical assumptions. We are interested here in 'finite' two-dimensional layers, i.e. a fluid strip that occupies a finite segment $0 < x < L$ along the wall, while being of infinite extent in the z -direction perpendicular to the plane of flow. There is some interest in finite three-dimensional layers, and also in layers that extend indefinitely, the departure of the layer height from a uniform level then being of a wave-like character (King, Tuck & Vanden-Broeck, 1993).

In the following, we first derive the governing integro-differential equation for the layer shape, then discuss its properties near the end points where $h(x) \rightarrow 0$, then solve it numerically. Surface tension σ is included in the formulation of the integro-differential equation, but we present here numerical results only for the case when its effect is confined to a small meniscus of lengthscale $l = [\sigma/(\rho_w g)]^{1/2}$ near the leading edge, with $l \ll L$. Hence σ is neglected in computing the overall shape of the layer. The results display non-unique solutions at fixed wall angle.

There are several studies of isolated stationary water drops on plane inclined walls. Those studies where surface tension is dominant, such as for the sessile or pendant drop, have a long history, going back at least to Laplace (Princen 1969). A feature of thin drops supported against gravity by surface tension is that their wetted length L is limited by surface tension to take values comparable to the meniscus scale l (Tuck & Schwartz 1991).

Larger fluid masses, with $L \gg l$, need a supporting mechanism other than surface tension, and the mechanism assumed here is the shear stress provided by an air stream.

There have been few studies of such flows for finite layers, although the effect of air streams on thin films of infinite extent has often been studied for industrial application such as coating (e.g. Tuck & Vanden-Broeck 1984).

A study on drops that is relevant to the present model is that of Durbin (1988). Durbin treats a surface-tension-dominated regime, and the effect of the air stream is viewed as a cause for potential dislodgement of a stationary drop on a horizontal wall, gravity being ignored. In Durbin's model, the air is assumed inviscid, and hence the air stream provides a normal stress, but not a shear stress, and the liquid within the drop is assumed to be at rest. This model does not yield any dislodgement (or support against gravity, if gravity were included) unless some drag-inducing mechanism is provided in the air flow. Durbin assumes that a wake with a constant-pressure free-surface forms in the air flow beyond a certain separation point on the drop surface. Durbin's model leads to a singular integro-differential equation for the drop shape, which is linear because the motion in the drop is neglected. In the present model, we assume that the liquid layer is thin enough so that it does not cause the air-flow boundary layer to separate on its surface, but we provide an alternative drag mechanism via the shear stress exerted by this boundary layer.

2. Formulation

If T denotes the surface traction exerted by the air, then the lubrication equations for a thin layer of viscous fluid with a free surface give that for steady flow

$$\frac{3T}{2h} = \frac{d}{dx}[P - \sigma h''(x) + \rho_w gZ], \quad (2.1)$$

where $P(x)$ is the pressure exerted by the air, and Z is an 'upward' coordinate in the direction opposite to gravity, measured at the water surface $y = h(x)$.

Formal derivations of (2.1) have been given by authors such as Atherton & Homsy (1976) and Tuck & Vanden-Broeck (1984). In summary, if μ is the liquid's viscosity, the quantity (say $\bar{P}'(x)$) on the right-hand side of (2.1) is the net effective pressure gradient in the x -direction, which drives a local Poiseuille-Couette flow of zero net volume flux, and the velocity component parallel to the wall is

$$u = \frac{\bar{P}'(x)}{2\mu} [y^2 - \frac{2}{3}h(x)y]. \quad (2.2)$$

Then (2.1) follows immediately, by equating the imposed surface traction T to the shear stress $\mu \partial u / \partial y$ evaluated at the free surface $y = h(x)$.

The formal conditions for validity of (2.1) are the same as those for lubrication theory (Cameron 1966; Acheson 1990, p. 248), the most important of which is that the layer be thin, with $\epsilon \ll 1$, where ϵ is a measure of layer slope, i.e. $h'(x) = O(\epsilon)$. This condition allows us to use (2.2) locally, i.e. to ignore x -variations relative to y -variations, and also to ignore differences between tangential and x -directions at the free surface, etc. Lubrication theory also demands a Reynolds number low enough for inertia to be negligible in the slow flow of velocity magnitude $V = O(Th/\mu)$ within the layer, but this Reynolds number can be moderately large when measured in terms of the parameter ϵ ; thus $\rho_w VL/\mu \ll \epsilon^{-2}$ is adequate (Moriarty, Schwartz & Tuck 1991).

With a wall inclined at a general angle α to the horizontal as in figure 1, we should have $Z = x \sin \alpha + h(x) \cos \alpha$, but we now assume that the angle α to the horizontal is small, specifically $\alpha = O(\epsilon)$. Then $Z \approx x\alpha + h(x)$ and (2.1) states

$$3T/2h(x) = P'(x) - \sigma h'''(x) + \rho_w gh'(x) + \rho_w g\alpha. \quad (2.3)$$

Equation (2.3) can be used to determine $h(x)$ only if $P(x)$ can be related to $h(x)$. When $h'(x) = O(\epsilon)$ is everywhere small, which we assume, this can be done by thin-airfoil theory (Tuck 1991; Newman 1977, p. 179; Van Dyke 1964, p. 49), namely

$$P(x) = -\frac{\rho_A U^2}{\pi} \int_0^L \frac{h'(\xi) d\xi}{x-\xi}, \quad (2.4)$$

where U the air stream velocity, and the drop is assumed to have finite length L measured along the wall in the direction of air flow. The integral in (2.4) is a Cauchy principal value.

Combining (2.3) and (2.4) yields a nonlinear integro-differential equation, which can be scaled to the form

$$\frac{1}{h(x)} = -\lambda \frac{d}{dx} \int_0^1 \frac{h'(\xi) d\xi}{x-\xi} - Sh'''(x) + h'(x) + \gamma. \quad (2.5)$$

Here x has been scaled by L , and h by h_0 , where

$$h_0 = (3TL/2\rho_w g)^{\frac{1}{2}}. \quad (2.6)$$

The non-dimensional parameters in (2.5) are

$$\lambda = \rho_A U^2 / \pi L \rho_w g, \quad (2.7)$$

$$\gamma = (L/h_0)\alpha = \alpha/\epsilon \quad (2.8)$$

and

$$S = \sigma / \rho_w g L^2. \quad (2.9)$$

Note that $\gamma = O(1)$ when $\alpha = O(\epsilon)$, as assumed. The non-dimensional surface tension S is a Bond number, but is best thought of as the square of the ratio between the meniscus scale $l = [\sigma/(\rho_w g)]^{\frac{1}{2}}$ and the drop length L . In principle, we can solve (2.5) for arbitrary values of S , but shall present results here only for the case of interest with S small.

We can now give an explicit formula for our fundamental small parameter ϵ measuring the ratio between the layer thickness and the layer length, namely

$$\epsilon = h_0/L = (\frac{3}{4}\pi\lambda C_D)^{\frac{1}{2}}, \quad (2.10)$$

where C_D is the drag coefficient of the air flow over the wet wall, such that

$$T = \frac{1}{2}\rho_A U^2 C_D. \quad (2.11)$$

The drag coefficient C_D is assumed small, and we expect the parameter λ to be of unit order; hence (as required) the aspect ratio ϵ of the layer is small, of the order of the square root of the drag coefficient.

The parameter λ is proportional to the square of a Froude number constructed from the air speed U , the drop length L , and the effective gravity (scaled by the water-air density ratio), i.e.

$$\frac{U^2}{(\rho_w/\rho_A)gL} = \pi\lambda. \quad (2.12)$$

Fixing λ fixes the length of the drop, namely

$$L = \frac{1}{\pi\lambda} \frac{\rho_A U^2}{\rho_w g}. \quad (2.13)$$

However, λ is not available as an input to (2.5), but must be determined by the

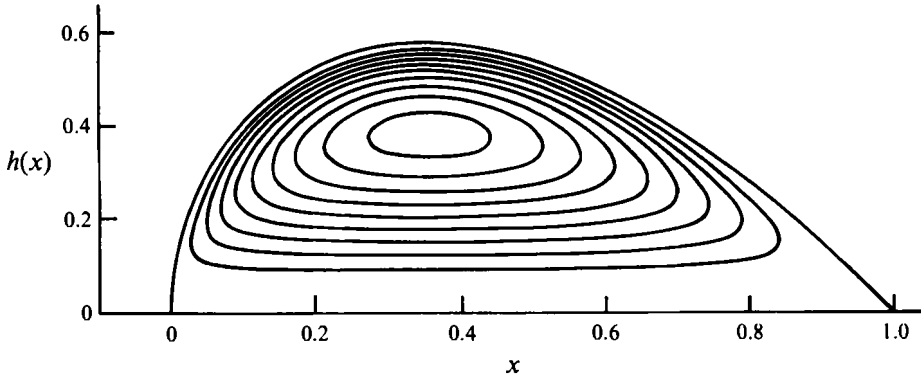


FIGURE 2. The computed layer shape and internal streamlines for a horizontal wall.

solution, in the manner of an eigenvalue; for example, at $\alpha = 0$ we find the (at least two-figure accurate) numerical value $\lambda = 0.40$, corresponding to the solution $h(x)$ shown in figure 2. That is, for arbitrary input λ , there is not necessarily a solution of (2.5) that vanishes at both ends. Any numerical solution technique must build-in simultaneous determination of this eigenvalue together with the unknown function $h(x)$.

3. End behaviour

At the ends of the drop, its thickness $h(x)$ must vanish, and hence the nonlinear term $1/h(x)$ in (2.5) becomes large. This large term must be balanced by at least one other large term in the equation, and the choice depends on whether the end under consideration is the upstream end $x = 0$ or the downstream end $x = 1$ of the air flow.

Consider first the downstream end $x = 1$. Then the balance here is between the lubrication force and the airflow pressure gradient, and $h(x)$ must tend linearly to zero, specifically as $x \uparrow 1$,

$$h(x) \approx \lambda^{-\frac{1}{2}}(1-x). \quad (3.1)$$

This behaviour yields a large positive contribution to the pressure gradient on the right-hand side of (2.5), which is therefore capable of cancelling exactly the singularity of the term in $1/h$. Thus the local shape of the tail of the drop is wedge-like; a corresponding wedge-like character to the nose $x = 0$ of the drop is impossible, since it yields a large negative pressure gradient. At such a wedge-like end with zero curvature, surface tension plays no essential role.

Note that the scaled slope at the downstream end is $h'(1) = -\lambda^{-\frac{1}{2}}$, which means that the actual contact angle β at that end is given by the small quantity

$$\beta = \lambda^{-\frac{1}{2}}\epsilon = \left(\frac{3}{4}\pi C_D\right)^{\frac{1}{2}}. \quad (3.2)$$

For some purposes it is convenient to introduce a parameter τ defined as the ratio between the wall angle and the downstream contact angle, i.e.

$$\tau = \alpha/\beta = \gamma\lambda^{\frac{1}{2}}. \quad (3.3)$$

The behaviour near the nose $x = 0$ is of a more singular nature. In the absence of surface tension, i.e. with $S = 0$, the only possibility is that the nose must be blunt, with infinite slope, i.e. as $x \downarrow 0$,

$$h(x) \approx (2x)^{\frac{1}{2}}. \quad (3.4)$$

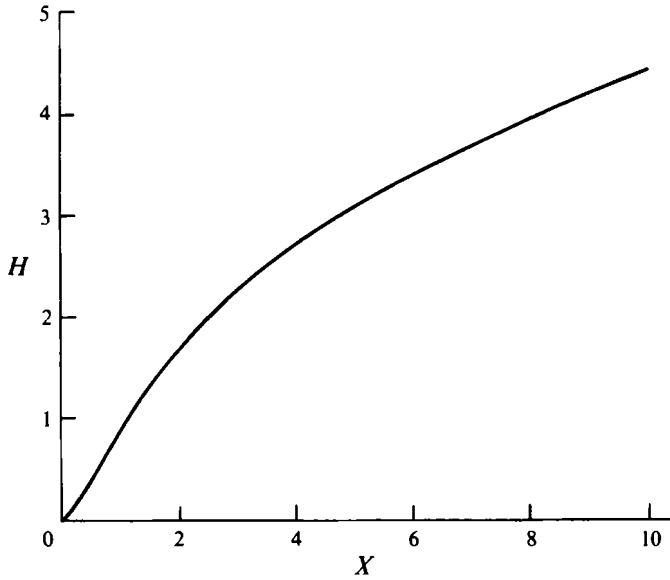


FIGURE 3. Shape of the meniscus layer near the leading edge.

The local force balance is then between the large lubrication and gravitational forces. The corresponding air-flow pressure gradient is bounded, and hence does not contribute to the leading-order local force balance. Note that thin-airfoil theory does not predict accurately the magnitude of this bounded pressure gradient near the nose for blunt-nosed bodies, but this is of no consequence for the leading-order force balance, which takes place between two larger terms.

This $h \approx x^{\frac{1}{2}}$ behaviour can extend right to the actual nose $x = 0$ only in the complete absence of surface tension, but the singularity is ameliorated locally by surface tension for small but non-zero S . The influence of surface tension is then confined to a meniscus region $0 < x < S^{\frac{1}{2}}$, where there is a three-way balance between surface tension, lubrication, and gravitational forces. This meniscus provides a transition between the outer apparent blunt nose, with $h(x)$ proportional to $x^{\frac{1}{2}}$, and the actual contact conditions at $x = 0$. For example, if S is small and we re-scale (2.5), setting

$$X = x/S^{\frac{1}{2}} \quad (3.5)$$

and

$$H = h/S^{\frac{1}{2}}, \quad (3.6)$$

we find that to leading order $H(X)$ must satisfy the nonlinear third-order ordinary differential equation

$$H''' - H' + H^{-1} = 0. \quad (3.7)$$

Figure 3 shows a numerical solution of this equation subject to $H(0) = H'(0) = 0$ and $H \approx (2X)^{\frac{1}{2}}$ as $X \rightarrow \infty$. This displays a smooth transition through the meniscus region where surface tension is important, from actual contact (at zero contact angle) to apparent contact (with $h \approx x^{\frac{1}{2}}$) in the outer region where surface tension is negligible. Since the only role of surface tension is to provide such a transition, and it does not influence the character or magnitude of the outer solution, we neglect surface tension in the following, setting $S = 0$ in (2.5), and using (3.4) to describe the leading-edge behaviour.

4. Numerical results

Our task is to solve the integro-differential equation (2.5) for $0 < x < 1$, with end behaviour of $h(x)$ at $x = 0$ given by (3.4), and at $x = 1$ by (3.1). Although (2.5) is most easily written in terms of the two parameters λ and γ , it is more convenient numerically to replace γ by the parameter τ defined in (3.3). One of the two parameters λ and τ can then be varied at will, while the other must be determined as part of the solution. Initially we assume that τ is given, and let the program determine $\lambda = \lambda(\tau)$. The singular behaviour of $h'(x)$ as $x \rightarrow 0$ will seriously degrade any conventional discretization of the integro-differential equation, and some manipulation prior to discretization is necessary.

We define a regularized layer elevation H on a graded mesh $y = x^{\frac{1}{2}}$, by $h = (2x)^{\frac{1}{2}}H(y)$, to obtain from (2.5)

$$H(y) \left[\lambda \frac{d}{dy} \int_0^1 \frac{H(s) + sH'(s)}{s^2 - y^2} ds + H(y) + yH'(y) + (2/\lambda)^{\frac{1}{2}}\tau y \right] - 1 = 0, \quad (4.1)$$

where now (3.1) and (3.4) imply

$$H \rightarrow 1 \text{ as } y \rightarrow 0 \text{ and } H \rightarrow (2\lambda)^{-\frac{1}{2}}(1 - y^2) \text{ as } y \rightarrow 1. \quad (4.2)$$

To avoid the computation of derivatives in (4.1), we further introduce the new variable $G(y) = H(y) + yH'(y)$, to obtain the regularized equation

$$\left[\int_0^y G(s) ds \right] \left[\lambda \frac{d}{dy} \int_0^1 \frac{G(s)}{s^2 - y^2} ds + G(y) + (2/\lambda)^{\frac{1}{2}}\tau y \right] - y = 0 \quad (4.3)$$

with $G(0) = 1$, $G(1) = -(2/\lambda)^{\frac{1}{2}}$.

Equation (4.3) is put into a form suitable for numerical solution by defining a mesh $y_i = i/n$ on $[0, 1]$ with the function $G(y)$ varying linearly on each interval $[y_i, y_{i+1}]$. This introduces n unknowns $G_1, G_2, \dots, G_{n-1}, \lambda$. By collocating (4.3) at the mid-points $y_{i+\frac{1}{2}} = (i + \frac{1}{2})/n$, $i = 0, 1, 2, \dots, n-1$, we obtain a system of n nonlinear algebraic equations of the form

$$\left[\sum_{j=0}^{i+\frac{1}{2}} w_j G_j \right] \left[\lambda T'(y_{i+\frac{1}{2}}) + G(y_{i+\frac{1}{2}}) + (2/\lambda)^{\frac{1}{2}}\tau y_{i+\frac{1}{2}} \right] - y_{i+\frac{1}{2}} = 0. \quad (4.4)$$

where w_j are suitable (modified trapezoidal) weights for numerical integration, and

$$T(y) = \sum_{j=0}^{n-1} \left[\frac{G_j - j(G_{j+1} - G_j)}{2y} \log \left| \frac{(y_{j+1} - y)(y_j + y)}{(y_{j+1} + y)(y_j - y)} \right| + \left(\frac{G_{j+1} - G_j}{2/n} \right) \log \left| \frac{y_{j+1}^2 - y^2}{y_j^2 - y^2} \right| \right]. \quad (4.5)$$

The quantities $T'(y_{i+\frac{1}{2}})$ and $G(y_{i+\frac{1}{2}})$ were evaluated by central differences, and the resulting system of algebraic equations was solved by a Powell method using the routine COSNBF from the NAG library. This method uses a combination of the Newton and steepest-descent iterations. The initial guess was taken to be a linear function on $[0, 1]$. This was successful for $0 \leq \tau \leq 0.40$, and a solution with residual error of less than 10^{-10} was produced with only a few iterations with $n = 60$. When n is increased beyond 60, the results are unchanged to at least two decimal places. For $\tau > 0.40$, a continuation method, with a previous converged numerical solution used as a starting value, was employed. No solutions were found by this technique for $\tau > 0.46$.

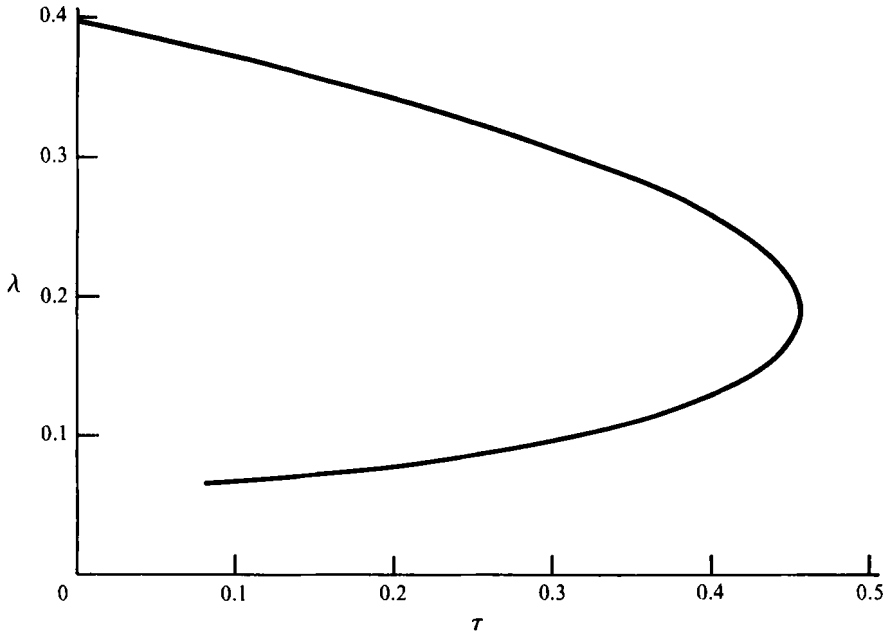


FIGURE 4. The computed relationship between the parameters λ (a measure of the airflow pressure) and τ (a measure of the wall angle).

Instead, in order to continue the computations, the parameter λ was specified and the computer procedure evaluated τ as an eigenvalue instead of λ .

A graph of the layer shape for $\tau = 0$ (i.e. a horizontal wall) is shown in figure 2. The corresponding computed value of λ is 0.40. The internal streamlines, calculated by a method given in the Appendix, are also shown. The existence of a clockwise rotating flow as indicated by the closed streamlines is clearly demonstrated.

The layer profile was found to change smoothly as τ increased up to the value 0.46. The shape near to this upper limit is actually that shown in figure 1, and the solution yields $\lambda = 0.19$. When the eigenvalue problem was reversed, i.e. when λ was specified, it was possible to find solutions for $0.19 > \lambda > 0.06$, and τ decreases from 0.46 in that range to about $\tau = 0.08$. Thus, at fixed τ (and hence at fixed γ) we have demonstrated a non-uniqueness of solutions, at least in the range $0.08 < \tau < 0.46$. This non-uniqueness is illustrated by the graph of λ versus τ in figure 4. There is a strong suggestion from this graph, because of the smooth merger of the two branches, that there are no solutions for $\tau > 0.46$; in any case, we have not been able to find any. If so, this means that there is an upper bound

$$\alpha < 0.46\beta = 0.70 C_D^{\frac{1}{2}} \quad (4.6)$$

(using (3.2), (3.3)) on the wall angle, above which steady solutions cannot exist. One should thus expect to observe apparently stationary drops on sloping walls only at or below this angle.

For $\tau < 0.46$, we have two solutions. We have been able to compute the solution branch with smaller λ only for $\tau > 0.08$, but this branch might well extend to lower values of τ and λ . There does, however, seem to be a suggestion in figure 4 that λ might not tend to zero with τ . Meanwhile, which one (if either) of the two solutions for $0.08 < \tau < 0.46$ is physically acceptable? This may be a stability matter, and is left for further work. However, we feel that the upper branch (higher λ) of figure 4 is more

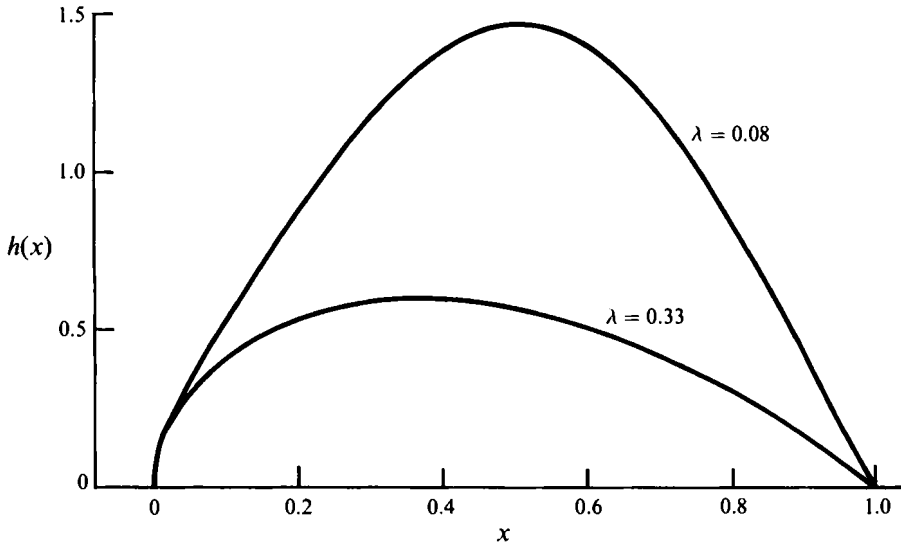


FIGURE 5. Layer shapes at $\tau = 0.23$, showing the two branches, namely $\lambda = 0.33$ and 0.08 .

promising, in part because it corresponds to thinner layers, where the viscous energy dissipation will be smaller. Figure 5 shows the two distinct solutions, with $\lambda = 0.33$ and 0.08 , at $\tau = 0.23$.

This work was done during a visit by A.C.K. to Adelaide. We thank the Royal Society and the Australian Research Council for support of this research.

Appendix. Internal streamlines

It is consistent with the lubrication equations that there is a stream function

$$\psi(x, y) = \frac{T}{4\mu} \left(\frac{y^3}{h(x)} - y^2 \right) \quad (\text{A } 1)$$

for the rotational flow in $0 \leq y \leq h(x)$, where T is the surface traction and μ the fluid viscosity. This stream function satisfies $\psi = 0$ on the wall $y = 0$ and also on the free surface $y = h(x)$, while taking negative values in $0 < y < h(x)$, with a local minimum of magnitude $-Th(x)^2/(27\mu)$ at $y = \frac{2}{3}h(x)$. Suppose $h = h_m$ at $x = x_m$ is the maximum layer thickness. Then the absolute minimum of the stream function occurs at this station $x = x_m$, namely $\psi_m = -Th_m^2/(27\mu)$.

A universal non-dimensional equation for the streamlines is therefore $\Psi = \text{constant}$, where

$$\Psi = \frac{27}{4} H^2 (Y^2 - Y^3) \quad (\text{A } 2)$$

and $\Psi = \psi/\psi_m$, $H = h/h_m$, and $Y = y/h$. All three scaled quantities Ψ , H , and Y in (A 2) lie between 0 and 1. The streamline $\Psi = 0$ is the wall plus the free boundary. The 'streamline' $\Psi = 1$ reduces to the single point $x = x_m$, $y = \frac{2}{3}h_m$, which is the centre of the counterclockwise vortex within the layer.

Any streamline $\Psi = \text{constant}$ defines a closed loop lying between two stations x where $H = \Psi^{\frac{1}{2}}$. For example, the streamline $\Psi = \frac{1}{4}$ has its lateral extremities at stations x where the layer thickness $h(x)$ has fallen to one-half of its maximum value h_m . The

vertical (normal to wall) extremities of these loops always occur at the station $x = x_m$ of maximum layer thickness, and at values Y that are solutions of the cubic equation (A 2) for $H = 1$.

All of the above considerations apply to elongated lubricating layers irrespective of the actual shape of the boundary $h(x)$ of the layer. For each value of Y , (A 2) is an explicit formula for $H = H(Y)$ on any streamline $\Psi = \text{constant}$. If now we are given a specification of $h(x)$, as for example is obtained in the text by numerical means, then this determines the actual streamline shape as follows. For each Y , we know $h(x) = h_m H(Y)$, and hence can read off a corresponding value of x from the output $h(x)$ data. Then we can plot the point (x, y) on this streamline, where $y = h(x) Y$, and repeat for all values of Y in the range $0 < Y < 1$. For simple convex layer shapes $y = h(x)$ as in the present paper, each value of Y in fact yields two points on the streamline, one fore and one aft.

REFERENCES

- ACHESON, D. J. 1990 *Elementary Fluid Dynamics*. Clarendon.
- ATHERTON, R. W. & HOMSY, G. M. 1976 On the derivation of evolution equations for interfacial waves. *Chem. Engng. Commun.* **2**, 57.
- CAMERON, A. 1966 *Principles of Lubrication*. Longmans.
- DURBIN, P. A. 1988 On the wind force needed to dislodge a drop adhered to a surface. *J. Fluid Mech.* **196**, 205–222.
- KING, A. C., TUCK, E. O. & VANDEN-BROECK, J.-M. 1993 Air-blown waves on thin viscous sheets. *Phys. Fluids A* **5**, 973–978.
- MORIARTY, J. A., SCHWARTZ, L. W. & TUCK, E. O. 1991 Unsteady spreading of thin liquid films with small surface tension. *Phys. Fluids A* **3**, 733–742.
- NEWMAN, J. N. 1977 *Marine Hydrodynamics*. MIT Press.
- PRINCEN, H. M. 1969 The equilibrium shape of interfaces, drops, and bubbles. In *Surface and Colloid Science* (ed. E. Matijevic & F. Eirich), vol. 2, pp. 1–84. Interscience.
- TUCK, E. O. 1991 A criterion for leading-edge separation. *J. Fluid Mech.* **222**, 33–37.
- TUCK, E. O. & SCHWARTZ, L. W. 1991 Thin static drops with a free attachment boundary. *J. Fluid Mech.* **223**, 313–324.
- TUCK, E. O. & VANDEN-BROECK, J.-M. 1984 Influence of surface tension on jet-stripped continuous coating of sheet materials. *Am. Inst. Chem. Engng J.* **30**, 808–811.
- VAN DYKE, M. 1964 *Perturbation Methods in Fluid Mechanics*. Academic.